

Low temperature aqueous phase synthesis and optical property study of ZnSe/ZnS core/shell quantum dots

XING ZHANG^{*,a,b}, MING XU^{*,a}, CHUNMAN YU^b, HAO LU^b, YAOTIAN YU^b, XIAONAN XU^a

^aKey Laboratory of Information Materials of Sichuan Province & School of Electrical and Information Engineering, Southwest University for Nationalities, Chengdu 610041, P.R. China

^bChengdu Chemtide Technology Co., Ltd., Chengdu 610041, P.R. China

High-quality ZnSe/ZnS core/shell nanocrystals were synthesized by a convenient aqueous phase method, achieving epitaxial growth at a very low temperature of 90°C. The nature of the ZnS shells grown on the surfaces of ZnSe core nanocrystals (average size, 4–5 nm) was determined by X-ray diffraction (XRD), UV-Vis spectrophotometry, photoluminescence (PL) measurements, high-resolution transmission electron microscopy (HR-TEM), and Fourier transform infrared spectroscopy (FT-IR). The PL intensity of ZnSe/ZnS quantum dots (QDs) first increased and then decreased with increasing pH value. The strongest PL intensity occurs at the pH value of ~10.5. The strongest PL peak was centered at 400 nm (FWHM ~22 nm). The mechanism of the observed optical properties is discussed.

(Received February 15, 2015; accepted June 24, 2015)

Keyword: Low temperature, pH, Quantum dots, Aqueous phase synthesis, Core-shell structure

1. Introduction

Quantum dots, each composed of a small number of atoms, are quasi-zero-dimensional nanomaterials, the size of which is between bulk materials and molecule materials. The quantum confinement effect in quantum dots is especially significant because internal electronic motion is limited in all directions. Quantum dots have been employed as a new class of fluorescent probes in many biological and biomedical applications, such as cellular imaging, solar cells and medical diagnostics [1-4], because of their size-dependent optical properties. At present, CdSe, CdS, CdTe quantum dots and so on have been widely studied [5-11] and exhibit very high luminous efficiency. However, the application of these quantum dots has been restricted by the toxicity of cadmium. To avoid the use of these toxic compounds, ZnSe has been proposed. It is an attractive semiconductor material with a band gap of 2.68 eV in the violet and blue region of the electromagnetic spectrum, and much less toxic than cadmium compounds, so it can be a useful material in several applications, such as blue light-emitting diodes [12], buffer layers for infrared detectors [13], or the first unit in a tandem solar cell [14].

As is well known, quantum dots nanocrystals synthesized by pyrolyzing organo-metallic reagents in hot organic solvents [15, 16] showed poor stability and low photoluminescence in earlier studies. Furthermore, organo-metallic compounds are toxic, expensive, and harmful to the environment, and their synthesis requires

high temperatures (up to 380°C) [17-19]. Aqueous phase synthesis is considered very important because it involves no toxins, uses cheap agents, and it is simple in operation, environment-friendly, low-temperature and easy to scale up to industrial production [20, 21]. Moreover, water resources are comparatively abundant in nature and the low-temperature synthesis process requires little energy. In order to improve quantum dots' stability and PL emission efficiency, the higher band gap inorganic shell ZnS (3.6 eV) has been epitaxially grown around the lower band gap core ZnSe (2.68 eV) nanocrystals. Through this method, high quality so-called type-I core/shell systems [22-24] have been obtained.

In the present work, high-quality ZnSe/ZnS core/shell nanocrystals were obtained through convenient aqueous phase synthesis using the epitaxial growth method at an uncommonly low temperature of 90°C. Luminescence performance has been optimized by varying reaction parameters. The luminescence performance, which is influenced by the ZnS shell and the pH value of the reaction solution of the ZnSe/ZnS quantum dots, is discussed in detail.

2. Experiment

2.1 Chemicals

All chemicals were analytical grade or the highest purity available. All solutions were prepared with

deionized water. Reagents – selenium power (~100 mesh) 99.9% trace and basis, NaBH_4 (96.0%, AR), $\text{Zn}(\text{AC})_2 \cdot 2\text{H}_2\text{O}$ (99%, AR), 3-mercaptopropionic acid (MPA, $\geq 99.0\%$) – were purchased from Sinopharm Chemical Reagent Co., Ltd (China).

2.2 Synthesis of ZnSe/ZnS core/shell quantum dots

In this typical synthesis, $\text{Zn}(\text{AC})_2 \cdot 2\text{H}_2\text{O}$ (1.319g) and deionized water (50 ml) were put into a three-necked flask and vigorously stirred for 30 minutes. Then mercaptopropionic acid was put into the above solution and the pH value was set from 8.5 to 13.5 by using 0.1 mol/L NaOH, so as to obtain zinc stock solutions. Meanwhile, selenium power, NaBH_4 and deionized water were mixed in an ice bath under the protection of argon atmosphere for 30 minutes, stirring in the process; thus we obtained transparent NaHSe solution. Selenium stock solution was quickly injected into the three-necked flask vessel, stirring for 50 minutes at 90°C in a water bath, yielding the ZnSe quantum dots solution.

Another batch of zinc stock solution was prepared using the same method. Hydrogen sulfide gas was prepared from ferrous sulfide and sulfuric acid (30%) under argon atmosphere, and then the argon gas carried the hydrogen sulfide into a mixed solution prepared from the zinc stock solution and the ZnSe quantum dots solution, after which the product was stirred for 70 minutes at 90°C in water bath. In this procedure the zinc ions and sulfide ions form a monolayer shell ZnS on the surface of ZnSe quantum dots. Flocculent precipitate was yielded when glycol was put into ZnSe/ZnS colloidal solution, then centrifuged, and dried in vacuum oven at 60°C , the purpose of which was to test the infrared spectrum and X-ray diffraction.

2.3 Characterization methods

The X-ray diffraction (XRD) was investigated with a diffractometer (Dandong Fangyuan Instrument LLC, DX-2500) using Cu $K\alpha$ radiation ($\lambda = 1.5405 \text{ \AA}$). High resolution transmission electron microscopy (HR-TEM) micrographs were investigated by using a field emission scanning electron microscope (JEOL, JSM-7500F). Optical absorption was measured in the 200-600 nm range using a UV/Vis spectrometer (Perkin Elmer Inc., Lambda-950). Photoluminescence spectra were performed with a spectrofluorophotometer (SHIMADZU, RF-5301PC), the excitation wavelength was 300 nm. All optical measurements were performed at room temperature under ambient conditions.

3. Results and discussion

ZnSe/ZnS quantum dots were prepared by aqueous phase synthesis at a low temperature of 90°C . In spectrofluorophotometry, the surface microenvironment

of the nanoparticles is indicated by the intensity of the fluorescent signal – using different wavelengths of light can excite quantum dots to fluoresce. Fig. 1 shows photoluminescence spectra of ZnSe (a) and ZnSe/ZnS (b) quantum dots; the excitation wavelength is 300 nm.

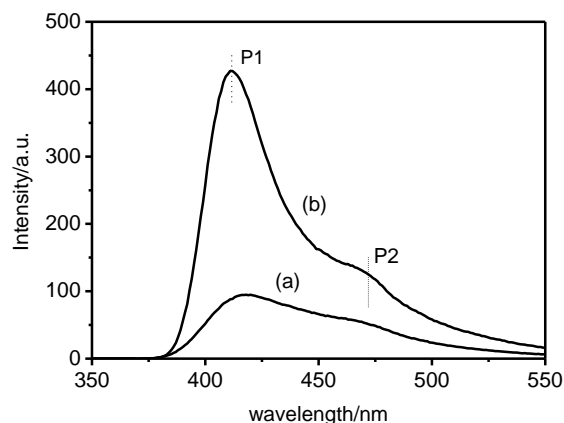


Fig. 1. Photoluminescence spectra of ZnSe (a) and ZnSe/ZnS (b) quantum dots. The excitation wavelength is 300nm.

It can be seen when a ZnS shell has been wrapped around the surface of a ZnSe core, the photoluminescence intensity of the particle increases significantly. There are two fluorescent peaks, the peak at 410 nm is intrinsic excitation luminescence; another peak 470 nm is due to the surface states emitting light generated by surface defects trapping carriers [25]. Surface defects of ZnSe are reduced owing to surface ZnS coating, which passivates the ZnSe surface defects. The carriers of ZnSe are kept inside the core because the band gap of ZnS is higher than that of ZnSe [26]. Consequently, the intensity of the excitonic luminescence spectra increases hugely after ZnS shell coated as shown in Fig. 1 (b).

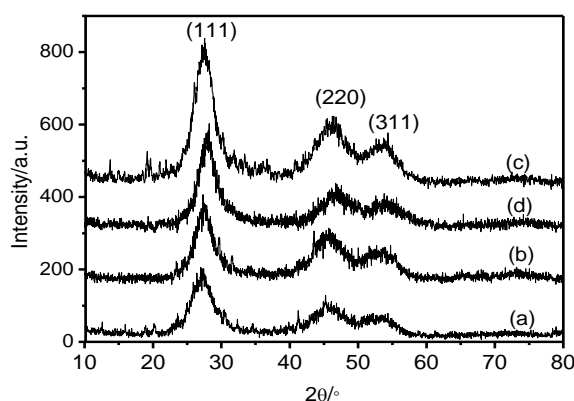


Fig. 2. XRD patterns of ZnSe (a) and ZnSe/ZnS (b,c,d) quantum dots with different pH values, (a,c) 10.5, (b) 8.5, (d) 13.5.

Fig. 2 shows XRD patterns of the uncoated ZnSe

particle and the ZnSe/ZnS quantum dots, respectively. All the samples grew preferentially along the (111) peak, accompanied by (220) and (311) crystal orientations, which indicates that those quantum dots consist of the characteristic cubic zinc blende [27]. The diffractive peaks of ZnSe are located at 27.8° , 46.4° , and 53.9° . The diffractive peaks of ZnSe/ZnS quantum dots shift to larger angles, located between the cubic ZnSe and ZnS phases. This is our initial evidence that the ZnS shell has wrapped the ZnSe core successfully, rather than forming a simpler combination of ZnS and ZnSe. From the XRD patterns it can be seen the diffractive peaks are broadened due to the finite crystal size. According to Debye-Scherrer formula, the grain size of ZnSe and ZnSe/ZnS quantum dots are about 3 nm and 4~5 nm respectively. Table 1 shows the detailed structural parameters of ZnS and ZnSe/ZnS quantum dots ($2\theta = 27.8^\circ$), further proof that the ZnS shell has wrapped the ZnSe core successfully.

Table 1. Structural parameters of ZnSe and ZnSe/ZnS quantum dots with different pH values, obtained from the XRD patterns in Fig. 2.

pH	(111) d/nm	FWHM/rad	D/nm
a: 10.5	0.3252	0.0524	2.958
b: 8.5	0.3234	0.0440	3.523
c: 10.5	0.3229	0.0351	4.416
d: 13.5	0.3234	0.0409	3.790

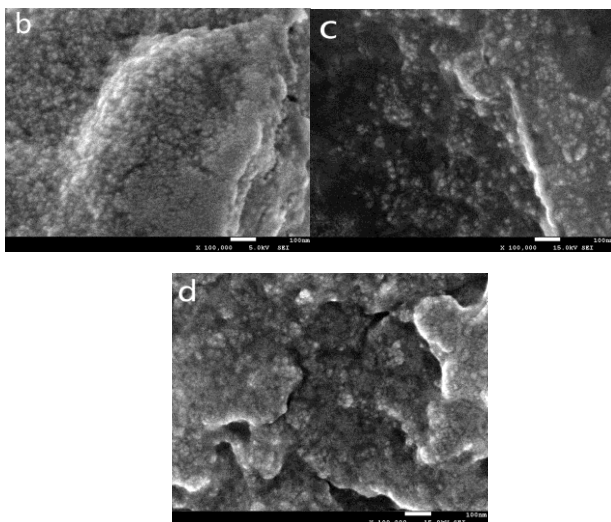


Fig. 3. SEM images of ZnSe/ZnS quantum dots with different pH values, (b) 8.5, (c) 10.5, (d) 13.5.

In addition, the pH value of the solution has a great

influence on the ZnSe/ZnS quantum dots. An appropriate alkaline environment favors the formation of the quantum dots, as evidenced by the XRD results. The diffraction peaks of ZnSe/ZnS quantum dots are the strongest, indicating that the ZnS shell has wrapped the ZnSe core, forming the core/shell quantum dots. Fig. 3 shows SEM images of ZnSe/ZnS quantum dots with different pH values. It can be seen that the nanoparticles have formed with mild agglomeration. The agglomeration phenomenon becomes more prominent with increasing pH value, indicating once again that pH value is a very important parameter in the preparation of ZnSe/ZnS quantum dots.

HRTEM micrographs of ZnSe/ZnS quantum dots are given in Fig. 4, clearly confirming the formation of a ZnS shell around the ZnSe core. The average diameter of these ZnSe/ZnS core/shell quantum-dot colloidal nanoparticles is about 4~5 nm.

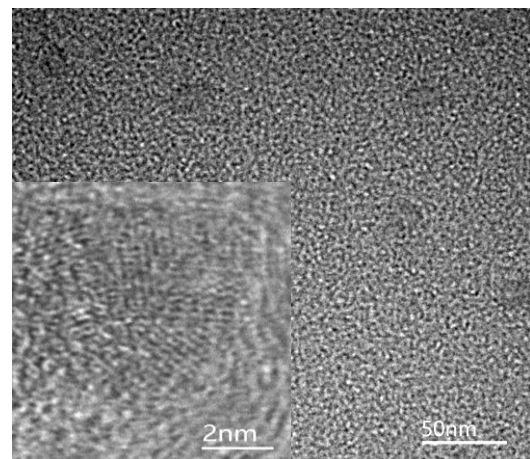


Fig. 4. HRTEM micrographs of ZnSe/ZnS quantum dots.

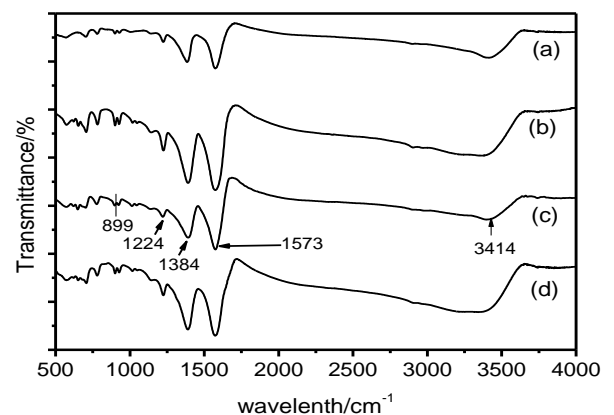


Fig. 5. FT-IR spectra of ZnSe (a) and ZnSe/ZnS (b,c,d) quantum dots with different pH values, (a,c) 10.5, (b) 8.5, (d) 13.5.

FT-IR spectra of ZnSe (a) and ZnSe/ZnS (b,c,d)

quantum dots with different pH values are displayed in Fig. 5. The vibration peak at 1573 cm^{-1} is assigned to the vas C=O stretching, whereas the band at 1384 cm^{-1} is due to the symmetric stretching ν_s C=O. The vibration peak at 3414 cm^{-1} and 899 cm^{-1} are due to the O-H stretching. Meanwhile, in comparison with the spectrum of MPA [26], the prominent characteristic peaks at 2923 cm^{-1} (C-H) and in the region from 2573 cm^{-1} to 2666 cm^{-1} (S-H) have practically disappeared, which suggests that MPA molecules attach to quantum dots through chemical bonding between thiols and dangling Zn atoms of the ZnSe layer [28]. S-H is adsorbed from MPA onto the ZnSe particles' surface in the form of a close-packed monolayer. Currently, the most exciting application of these particles is in treating dye-bearing wastewater. The interaction of cationic dye molecules and the negatively charged quantum dots promotes degradation of the dyes, mediated by OH radicals or a redox reaction on the quantum dots' surface, so ZnSe/ZnS quantum dots can exist stably in water solution.

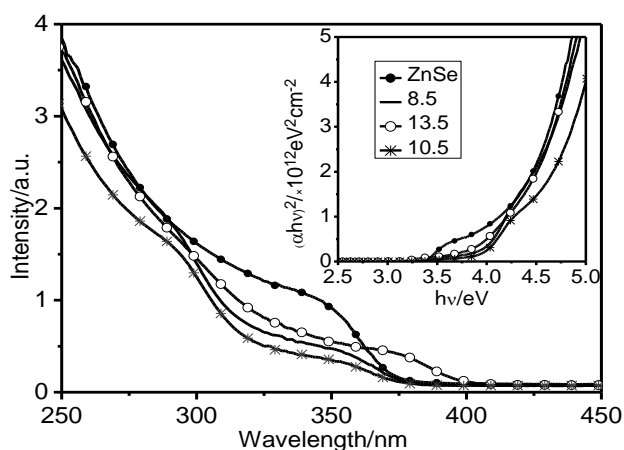


Fig. 6. Absorption spectra of ZnSe/ZnS quantum dots synthesized under different pH values, (b) 8.5, (c) 10.5, (d) 13.5. Inset shows the curve of $(\alpha h\nu)^2$ vs $h\nu$ for ZnSe/ZnS quantum dots.

Absorption spectra of ZnSe/ZnS synthesized under different pH values are given in Fig. 6. A broad absorption peak at about 330 nm can be observed; there is an obvious regular modulation of optical absorption as the pH value is increased. The optical energy band gap of ZnSe nanoparticles is calculated using Tauc's formula [29]

$$\alpha = \frac{B(h\nu - E_g)^n}{h\nu}$$

where the exponent n could have the values of 0.5, 1.5, 2 and 3 for four transitions – direct allowed, direct forbidden, indirect allowed, and indirect forbidden – depending on the type of electronic transition occurring

in k -space. For ZnSe, the transition is “direct allowed,” so $n = 0.5$. The band gap is determined by extrapolating the linear region of $(\alpha h\nu)^2 \sim h\nu$ plots, as showed in Fig. 6 (inset). The value of the band gap E_g for ZnSe is 3.3 eV, larger than 2.7 eV for bulk ZnSe, which is characteristic of the quantum confinement effect. The pH value has a pronounced effect on the optical band gap, contrary to the published findings of some former earlier research [30]. The effect might be caused by the different thickness of the ZnS layer grown on the surface of ZnSe and the number of OH radicals (see Fig. 5).

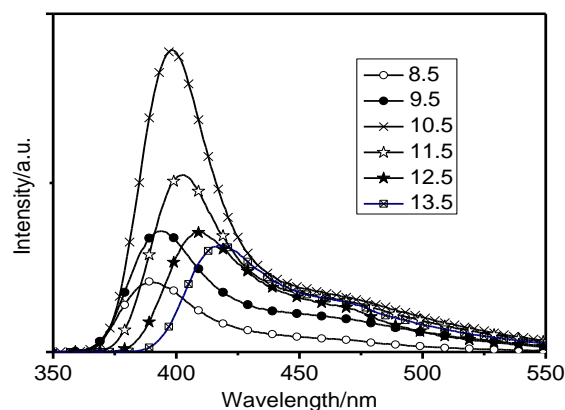


Fig. 7. Photoluminescence spectra of ZnSe/ZnS quantum dots synthesized at different pH values. The excitation wavelength is 300nm.

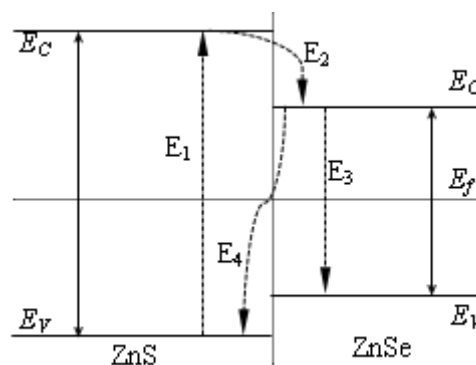


Fig. 8. Energy band diagram of ZnSe/ZnS core/shell nanocrystals.

We further investigated the stability of ZnSe/ZnS quantum dots synthesized at different pH values in order to determine the effects of aquatic conditions on the synthesized particles. PL spectra of ZnSe/ZnS quantum dots under different pH value are shown in Fig. 7; the excitation wavelength is 300 nm. The PL intensity first increases and then decreases with increasing pH value. The maximum PL intensity corresponds to the pH value of 10.5; the high emission peak is centered at 400 nm (FWHM ~ 22 nm), which is attributed to the ZnS shell

packed onto the ZnSe core. Meanwhile, the peak wavelength increases with the increase of pH value. According to Derjagui-Landan and Verwey-Overbeek theory [31, 32], the interaction balance between the van der Waals attractive force and the electrostatic repulsive force determines the stability of the quantum-dot colloidal solution. When the pH value changes from 8.5 to 10.5, the dissociation reaction of thiol functional groups plays a key role in the surface potential of colloidal nanoparticles [33-35]. As the pH value increases to 13.5, the thickness of ZnS and the number of OH radicals play key roles in the surface properties of the ZnSe/ZnS nanoparticles.

Fig. 8 shows the energy band of the ZnSe/ZnS core/shell structure, which is a Type-I structure wherein the shell possesses a higher conduction band and a lower valence band than those of the core, so the photo-generated carriers are mostly confined inside the core [36]. In Type-I structured nanocrystals, excited electrons cross from the valence band of the shell and core to the conduction band of shell. In fact, the transfer of an electron from the conduction band of the shell to the conduction band of the core takes only several picoseconds, much quicker than the few hundred picoseconds required for an electron and a hole inside the shell to recombine [37]. So almost all electrons in the conduction band of ZnS transfer to the conduction band of ZnSe very quickly (E2, in Fig. 2), and then combine with holes in the valence band of ZnS and ZnSe (E3 and E4). During the process of combination, the theoretical energy released corresponds to peaks P1 and P2 in Fig. 1, and P2 corresponds to the band edge emission. This process usually occurs in the interface between the ZnSe core and the ZnS shell, indicating that the ZnS shell was successfully grown on the ZnSe core.

4. Conclusions

In this paper, we reported the aqueous phase synthesis of ZnSe/ZnS core/shell environment-friendly nanocrystals using an epitaxial growth method at a very low temperature. The structural and optical properties of these quantum dots were found to be very dependent on the pH value, stabilizing agent, and so on. The growth of the ZnS shell on the surface of ZnSe core nanocrystals was verified by XRD, HRTEM, PL, FT-IR and UV-Vis. In view of these measurements, we determined that the pH value 10.5 was the best condition for growing ZnSe/ZnS core/shell quantum dots with an average crystallite size of 4~5 nm. In addition, we tested the quantum yield (QY) of the quantum dots – the maximum QY was obtained when the pH value was 10.5.

Acknowledgments

This work was financially supported by the Science and Technology Department of Sichuan Province, P.R.

China (2013GZ0098). It was also supported by Subject Construction Funds of Southwest University for Nationalities (Grant No. 2015XWD-S0805), PR China.

References

- [1] B. Dubertret, P. Skourides, D. J. Norris, V. Noireaux, A.H. Brivanlou, A. Libchaber. *Science*, **298**, 1759 (2002).
- [2] W. C. W. Chan, S. Nie. *Science*, **281**, 2016 (1998).
- [3] R. E. Bailey, A. M. Smith, S. Nie. *Phys. E.*, **25** (1), 1 (2004).
- [4] S. A. Robinson, M. J. Lajeunesse, M. R. Forbes. *Environ. Sci. Technol. Lett.*, **46** (13), 7094 (2012).
- [5] C. S. Kim, M. Kim, J. K. Furdyna, M. Dobrowolska, S. Lee, H. Rho, L. M. Smith, H. E. Jackson, E. M. James, Y. Xin, N. D. Browning. *Phys. Rev. Lett.*, **85**, 1124 (2000).
- [6] M. Strassburg, Th. Deniozou, A. Hoffmann, R. Heitz, U.W. Pohl, D. Bimberg, D. Litvinov, Rosenauer, D. Gerthsen, S. Schwedhelm. *Appl. Phys. Lett.*, **76**, 685 (2000).
- [7] S. Kim, B. Fisher, H. J. Eisler. *J. Am. Chem. Soc.* **125** (38), 11466 (2003).
- [8] S. F. Wuister, I. Swart, F. Driel, S.G. Hickey, C. M. Donegá. *Nano Letters*, **3**(4), 503 (2003).
- [9] B. I. Lemon, R. M. Crooks, *J. Am. Chem. Soc.* **122** (51), 12886 (2000).
- [10] N. Soltani, E. Saion, M. Z. Hussein, M. Erfani, A. Abedini, G. Bahmanrokh, M. Navasery, P. Vaziri. *Int. J. Mol. Sci.* **13**(10), 12242 (2012).
- [11] Y. M. Guo, X. M. Shi, J. Zhang, Q. L. Fang, L. Yang, F. F. Dong, K. Wang. *Materials Letters*. **86** (1), 146 (2012).
- [12] N. Myoung, V. V. Fedorov, S. B. Mirov, L. E. Wenger. *J. Lumin.* **132**(3), 600 (2012).
- [13] F. Keilmann, C. Gohle, R. Holzwarth, *Optics Letters*, **29**(13), 1542 (2004).
- [14] Z. J. Ning, H. N. Tian, C. Z. Yuan, Y. Fu, H. Y. Qin, L. C. Sun, H. Ågren, *Chem. Commun.*, **47**, 1536 (2011).
- [15] Z. A. Peng, X. Peng. *J. Am. Chem. Soc.* **123**(1), 183 (2001)
- [16] Z. T. Deng, L. Cao, F. Q. Tang, B. S. Zou. *J. Phys. Chem. B.* **109**(35), 16671 (2005).
- [17] H. R. Pouretedala, A. Norozib, M. H. Keshavarza, A. Semnani. *J. Hazardous Materials*. **162**(2), 674 (2009).
- [18] Z. Y. Gao, N. Liu, D. P. Wu, W. G. Tao, F. Xu, K. Jiang. *App. Sur. Sci.* **258** (7), 2743 (2012).
- [19] T. Ghosha, J. H. Leeb, Z. D. Menga, K. Ullaha, C. Y. Parka, V. Nikama, W. C. Oha. *Materials Research Bulletin*. **48** (3), 1268 (2013).
- [20] Y. G. Kim, K. S. Baek, S. K. Chang. *Solid State Communications*. **149**, 937 (2009).
- [21] C. A. Smith, H. W. H. Lee, V. J. Leppert, S. H. Risbud. *Appl. Phys. Lett.* **75**, 1688 (1999).

- [22] Z. Y. Gu, L. Zou, Z. Fang, W.H Zhu, X.H. Zhong. *Nanotechnology*, **19**, 135604 (2008).
- [23] Y. Zheng, Z. Yang, J. Y. Ying. *Adv. Mater.*, **19**, 1475 (2007).
- [24] Z. Fang, L Liu, J Wang, X. H. Zhong. *J. Phys. Chem. C*. **113**(11), 4301 (2009).
- [25] X. G. Peng, M. C. Schlamp, A. V. Kadavanich, A. P. Alivisatos, *J. Am. Chem. Soc.*, **119** (30), 7019 (1997).
- [26] A. N. Luis, B. R. Sonia, C. A. Ricardo, P. P. Oscar, R. Felix, *J. Nanosci. Nanotech.*, **14**, 7333 (2014).
- [27] Y. L. Ding, H. D. Sun, D. Liu, F. T. Liu, D. Z. Wang. *Journal of the Chinese Advanced Materials Society*, **1**, 36(2013).
- [28] J. Ke, X. Y. Li, Y. Shi, Q. D. Zhao, X. C. Jiang. *Nanoscale*, **4**, 4996 (2012).
- [29] F. Wooten, *Optical Properties of Solids*, Academic Press Inc., 1972, p. 45.
- [30] J. Lee, *Thin Solid Films*, **516** (7), 1386 (2008).
- [31] D. Grasso, K. Subramaniam, M. Butkus, K. Strevett, J. Bergendahl. *Rev. Environ. Sci. Biotechnol.*, **1**(1), 17 (2002).
- [32] S. W. Bian, I. A. Mudunkotuwa, T. Rupasinghe. V.H. Grassian, *Langmuir*. **27**, 6059 (2011).
- [33] Z. Fang, Y. Li, H. Zhang, X. H. Zhong, L. Y. Zhu. *J. Phys. Chem. C*, **113** (32), 14145 (2009).
- [34] H. Zhang. Y. Liu, J. H. Zhang, H. Z. Sun, J. Wu, B. Yang. *Langmuir*, **24**(22), 12730 (2008).
- [35] Y. S. Li. F. L. Jiang, Q. Xiao, R. Li, K. Li, M. F. Zhang, A. Q. Zhang, S. F. Sun. *Appl. Catal. B: Environ.* **101**, 118 (2010).
- [36] J. J. Li, Y. A. Wang, W. J. Guo. *J. Am. Chem. Soc.*, **125** (41), 12567 (2003).
- [37] J. Puls, V. V. Rossin, F. Kreller, H. J. Wünsche, S. Renisch, N. Hoffmann, M. Rabe, F. Henneberger, *Journal of Crystal Growth*, **159**, 784 (1996)

*Corresponding author: zhangxingskt@126.com
hsuming_2001@aliyun.com